© 2015. Published by The Company of Biologists Ltd | The Journal of Experimental Biology (2015) 218, 858-863 doi:10.1242/jeb.115519

RESEARCH ARTICLE

Symbiont type influences trophic plasticity of a model cnidarian–dinoflagellate symbiosis

Miguel C. Leal[1,*], Kenneth Hoadley[2], D. Tye Pettay[2], Alejandro Grajales[3], Ricardo Calado[1] and Mark E. Warner[2]

ABSTRACT

The association between cnidarians and photosynthetic dinoflagellates within the genus *Symbiodinium* is a prevalent relationship in tropical and subtropical marine environments. Although the diversity of *Symbiodinium* provides a possible axis for niche diversification, increased functional range and resilience to physical stressors such as elevated temperature, how such diversity relates to the physiological balance between autotrophy and heterotrophy of the host animal remains unknown. Here, we experimentally show interspecific and intraspecific variability of photosynthetic carbon fixation and subsequent translocation by *Symbiodinium* to the model cnidarian host *Aiptasia pallida*. By using a clonal anemone line harboring different species of *Symbiodinium*, we determined that symbiont identity influences trophic plasticity through its density, capacity to fix carbon, quantity of translocated carbon and ultimately the host's capacity to ingest and digest prey. Symbiont carbon translocation and host prey ingestion were positively correlated across symbiont combinations that consisted of different isoclonal lines of *Symbiodinium minutum*, while a combination with type D4-5 *Symbiodinium* displayed lower carbon translocation, and prey capture and digestion more similar to *Aiptasia* lacking symbionts. The absence of a shift toward greater heterotrophy when carbon translocation is low suggests that the metabolic demand of feeding and digestion may overwhelm nutritional stores when photosynthesis is reduced, and amends the possible role of animal feeding in resistance to or recovery from the effects of climate change in more obligate symbioses such as reef-building corals.

KEY WORDS: *Symbiodinium*, Functional diversity, Nutrition, Photosynthesis

INTRODUCTION

Several animals thrive in oligotrophic environments, such as coral reefs, by capitalizing on the photosynthetically fixed carbon of endosymbiotic dinoflagellates (Venn et al., 2008). The association between coral reef cnidarians and dinoflagellates within the genus *Symbiodinium* represents one such key cosmopolitan symbiosis in the oceans (Coffroth and Santos, 2005; Weis et al., 2008). While the interspecific diversity and flexibility of *Symbiodinium* is well known (Coffroth and Santos, 2005; Sampayo et al., 2008), the intraspecific diversity as well as functional diversity of *Symbiodinium* and subsequent consequences for the nutritional balance of the cnidarian host remain unexplored. Symbiotic cnidarians rely on autotrophy, through the photosynthetically fixed carbon translocated by their symbionts, and heterotrophy, by feeding on planktonic organisms (Falkowski et al., 1984). In some cases, this trophic plasticity is critical for the resilience of these symbiotic associations (Grottoli et al., 2006). A shifting reliance from autotrophy to heterotrophy with light attenuation and depth is usually observed within different coral species (Muscatine et al., 1989; Anthony and Fabricius, 2000; Leal et al., 2014a). Heterotrophy may also affect the photosynthetic performance of the symbionts but have no consequence in terms of the total amount of carbon translocated to the host (Davy and Cook, 2001). In addition, autotrophy may be inversely related to heterotrophic contribution in response to stress events, such as bleaching or notable changes in light regime (Grottoli et al., 2006; Hughes and Grottoli, 2013; Tremblay et al., 2014).

Symbiont genotypic diversity affects the quantity and quality of translocated material to the host (Loram et al., 2007; Starzak et al., 2014), which ultimately has physiological consequences for symbiotic cnidarians and may contribute to the selective loss of cnidarian diversity (Grottoli et al., 2014). However, how symbiont diversity directly relates to the trophic plasticity of the holobiont (used here to simply refer to the animal and photosynthetic symbionts) remains unknown. Notably, no direct simultaneous comparisons exist between autotrophic and heterotrophic performance that account for symbiont identity in a genetically controlled host environment. Here, we address the consequences of interspecific and intraspecific variability of *Symbiodinium* and its relationship to the trophic plasticity of the association as defined by the interaction of autotrophic and heterotrophic performance. We hypothesized that symbiotic associations with low carbon translocated to the animal counterbalance such nutritional loss by increasing feeding and digestion. We used the sea anemone *Aiptasia pallida* (Agassiz in Verrill 1864) because of the considerable recent interest in using this model organism to understand the physiology and co-evolution of cnidarian–*Symbiodinium* symbioses (Weis et al., 2008; Thornhill et al., 2013). An isoclonal line of this symbiotic sea anemone *A. pallida* (line CC7) was used while individually hosting two isoclonal lines (i.e. strains 1 and 2) of its naturally occurring clade B symbiont (*Symbiodinium minutum*, ITS2 type B1), and a mixture of one *S. minutum* with a different symbiont within the clade B lineage (*Symbiodinium psygmophilum*, ITS2 type B2). A single isolate of *Symbiodinium* sp. from the putatively thermally tolerant clade 'D' lineage (ITS2 type D4-5) (Rowan, 2004; Lajeunesse et al., 2010a) was also used with the CC7 host. Additionally, we tested a different *A. pallida* line originally collected from Bermuda that hosted an additional unique strain of *S. minutum* (strain 3). Photosynthetic performance and carbon translocation by the symbionts to the host, together with host prey capture and digestion, provided the proxies to score nutritional plasticity of these symbioses. To gauge zooplankton capture (ingestion) and digestion alone, i.e. heterotrophic performance (Leal et al., 2014b), the results of feeding assays were compared with those from CC7 anemones lacking any symbionts (aposymbiotic).

[1]Departamento de Biologia & CESAM, Universidade de Aveiro, Campus Universitário de Santiago, Aveiro 3810-193, Portugal. [2]College of Earth, Ocean, and Environment, University of Delaware, Lewes, DE 19958, USA. [3]Department of Invertebrate Zoology, American Museum of Natural History, Central Park West at 79th Street, New York, NY 10024, USA.

*Author for correspondence (miguelcleal@gmail.com)

Received 15 October 2014; Accepted 8 January 2015

The Journal of Experimental Biology

The Journal of Experimental Biology (2015) 218, 858-863 doi:10.1242/jeb.115519

RESULTS

Overall, photosynthesis was a good predictor of carbon translocation to the animal when grouping all animal–dinoflagellate combinations, and a significant positive correlation was observed between the rate of carbon fixation (photosynthesis) and carbon translocation to the animal when normalized to *Symbiodinium* cell number (Fig. 1; Pearson correlation, N=25, r=0.89, t=9.368, d.f.=23, P<0.001). However, when comparing this pattern among different *Symbiodinium* genotypes, significant differences were noted, particularly in the CC7 anemone hosting the D4-5 symbiont, where carbon translocated per cell remained high across the range of photosynthesis (P<0.05; supplementary material Table S1). Substantial differences were observed in symbiont density (ANOVA, N=25, F=13.16, P<0.001), particularly between strain 3 and the D4-5 symbiont, which averaged 5057 and 1382 cells μg^{-1} protein, respectively (Table 1). Nevertheless, photosynthetic performance of each animal–dinoflagellate combination together with symbiont density resulted in greater carbon translocated to the host as *Symbiodinium* density increased (Pearson correlation, N=25, r=0.75, t=5.4352, d.f.=23, P<0.001). Carbon translocation significantly varied among symbiont genotypes (ANOVA, N=25, F=4.006, P<0.05), particularly between strain 2 and D4-5 symbionts, which averaged 1.09×10^{-7} and 3.14×10^{-7} µg C $cell^{-1}$ h^{-1}, respectively (Table 1). The positive correlation between symbiont density and carbon translocated was observed among the two symbiont clades and anemone lines (i.e. clade B versus D, and strain 3; supplementary material Table S1).

For all dinoflagellate–anemone combinations that contained *Symbiodinium* clade B, including the other anemone line hosting *S. minutum* (strain 3), there was a positive association between the rate of carbon translocation and prey ingestion (Fig. 2A). However, the D4-5 symbiosis had considerably lower rates of carbon translocation relative to the high rate of prey ingestion. Furthermore, significant interspecific and intraspecific differences were observed for prey ingestion and prey DNA breakdown (a proxy for prey degradation) among the different dinoflagellate–anemone combinations (Fig. 2B,C). In particular, a pattern of high prey ingestion rate and slow prey digestion was observed for aposymbiotic individuals (lacking symbionts) and anemones hosting the D4-5 symbiont (supplementary material Table S2). This pattern was also noted for the other anemone line hosting a different genotype of *S. minutum* (strain 3; Fig. 2B,C).

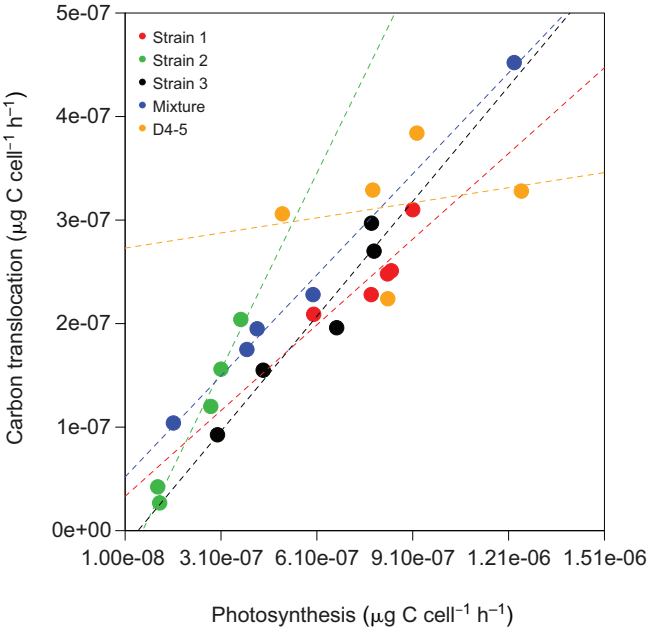

Fig. 1. Relationship between maximal photosynthesis and carbon translocation to the host. Photosynthesis and carbon translocation rates were normalized to *Symbiodinium* cell number in individual *Aiptasia pallida* hosting a single unique strain of *Symbiodinium minutum* (denoted by strain 1, 2 or 3), a 'mixture' of *S. minutum* strain 2 and *Symbiodinium psygmophilum*, or D4-5 (N=5 per *Symbiodinium* genotype combination). Dashed lines correspond to a linear fit for each strain. Symbioses with strains 1, 2, 'mixture' and D4-5 were all with the same clonal (CC7) anemone line.

DISCUSSION

This study shows that the genetic identity of *Symbiodinium* influences the nutritional plasticity of a cnidarian–dinoflagellate symbiosis. The marked differences between host prey feeding and digestion are associated with both photoautotrophic carbon translocation and symbiont type, even at the symbiont sub-species level. Notable differences in symbiont density and the resulting variability in carbon translocation among *Symbiodinium* strains within *S. minutum* alone underscore the functional diversity within these dinoflagellates, the intraspecific variability within a single *Symbiodinium* species, and that broad physiological generalizations for entire clades of *Symbiodinium* (e.g. Fabina et al., 2013) are likely not warranted.

We hypothesized that symbiotic associations with lower autotrophic contribution (i.e. less carbon translocated to the animal) would compensate for such losses by increasing feeding and digestion (Grottoli et al., 2006; Ferrier-Pagès et al., 2011; Hughes and Grottoli, 2013). However, the results suggest that higher autotrophy is strongly associated with increased heterotrophy, apart from the D4-5 symbiont, which did not fit this pattern (Fig. 2A). The association with the D4-5 symbiont resulted in relatively low total carbon translocated but high prey ingestion (Fig. 2A). Likewise, aposymbiotic anemones rely on prey capture and ingestion efforts as their only source of nutrients (Grottoli et al., 2006; Leal et al., 2013). Similar prey ingestion and digestion between aposymbiotic *Aiptasia* and anemones hosting D4-5 symbionts (Fig. 2B,C) suggests that both groups of anemones increase their heterotrophic efforts through prey capture and ingestion but subsequent prey breakdown and digestion are relatively slow. While the high prey gut content of these anemones (Fig. 2B) may justify their slow digestion rates (supplementary material Table S2), the similarity between the aposymbiotic and clade D-harboring anemones may also be explained by the reduced autotrophic contribution of D4-5 symbionts to support host metabolism and, particularly, physiological costs associated with prey digestion (Sebens, 2002). These results are in contrast to those of Hiebert and Bingham (2012), who noted no significant difference in the feeding ability of the temperate anemone *Anthopleura elegantissima* while aposymbiotic or harboring *Symbiodinium* or 'zoochlorellae'. While not measured here, it is also possible that symbiont type in *Aiptasia* affects the anemone's capacity to capture prey through morphological variations such as tentacle number, size or cnida characteristics (Hiebert and Bingham, 2012).

Carbon fixation and translocation varied among *Symbiodinium* genotypes (Table 1). However, the similar trends observed across genotypes between photosynthesis and carbon translocation, and between *Symbiodinium* density and carbon translocation suggest a similar autotrophic mechanism among strains of the same species (*S. minutum*) and regardless of anemone line. The results also suggest that differences in *Symbiodinium* density affect the congruence between high carbon fixation and translocation per

The Journal of Experimental Biology (2015) 218, 858-863 doi:10.1242/jeb.115519

Table 1. Photobiological characteristics of individual *Aiptasia pallida* hosting a single unique strain of *Symbiodinium minutum*, a mixture of *S. minutum* and *S. psygmophilum*, or D4-5

Parameter	Strain 1	Strain 2	Strain 3	Mixture	D4-5
Symbiodinium cell density (cells μg^{-1} protein)	2778±958^{a}	2544±328^{a,b}	5057±827^{c}	1883±522^{a,b}	1382±116^{b}
Photosynthesis (10^{-7} μg C $cell^{-1}$ h^{-1})	7.92±1.17^{a,b}	2.38±1.17^{c}	5.96±2.17^{b,c}	5.60±4.04^{b,c}	8.54±2.69^{b}
Carbon translocation (10^{-7} μg C $cell^{-1}$ h^{-1})	2.49±0.38^{a,b}	1.09±0.75^{b}	2.02±0.84^{a,b}	2.31±1.31^{a,b}	3.14±0.58^{a}
Total carbon translocation (10^{-4} μg C μg^{-1} protein h^{-1})	6.1±2.9^{AB}	3.5±1.8^{a}	11.0±4.4^{b}	4.4±2.5^{a}	5.1±4.1^{a,c}

Strain, *A. pallida* hosting a single unique strain (1, 2, or 3) of *Symbiodinium minutum*; Mixture, *S. minutum* strain 2 and *S. psygmophilum*.
Data are means±s.d., *N*=5 per *Symbiodinium* genotype combination. Different superscript letters in the same row denote significant differences (P<0.05).

symbiont and total translocation to the host, as was observed in the anemones harboring the D symbiont (Fig. 1, Table 1; supplementary material Table S1). As a consequence of the low cell density of the D4-5 symbiont, increased photosynthetic rates are needed to translocate the same amount of carbon (Fig. 1). Symbiont cell density is determined, in part, by the photosynthetic carbon flux and individual metabolic requirements of symbionts, which vary with symbiont type (Dubinsky and Berman-Frank, 2001; Starzak et al., 2014). Although Davy and Cook (2001) have suggested that low symbiont density promotes high photosynthetic rates as a consequence of decreased competition for CO_2, the results recorded here show that symbioses supporting high *Symbiodinium* densities may also display relatively high photosynthesis, such as strain 3 (Table 1). Moreover, notably different photosynthetic rates were observed among closely related symbionts displaying similar cell density (strain 1 and 2; Table 1). It is, therefore, likely that a combination of the effects of symbiont type, symbiont density and anemone line affect photosynthetic rates. Further, possible space constraints or other as yet uncharacterized control elements of the animal and cellular recognition signals between the partners may play a defining role here (Schoenberg and Trench, 1980; Smith and Muscatine, 1999). The effect of symbiont type and density may be of particular importance in D4-5 symbionts, as low cell density is probably affecting total carbon translocation to the host. While the symbiosis with the D4-5 symbiont was stable, it may represent a suboptimal symbiosis between host and symbiont lineages that have not co-evolved. This may cause the strong relationship between autotrophy and heterotrophy noted in the other holobionts and across *S. minutum* genotypes to break down in this particular symbiosis (Fig. 2A). If true, this symbiont may be an inefficient competitor against homologous symbionts of *Aiptasia* such as *S. minutum*. While not measured in this study, a difference in the quality of translocated material between different symbiont types, as already noted in another tropical anemone harboring different clades of *Symbiodinium* (Loram et al., 2007), could also contribute to this trend and certainly warrants further study.

The positive association between autotrophy and heterotrophy for the different *S. minutum* strains and the anemone harboring the mixed clade B assemblage may be due to two non-mutually exclusive reasons: (1) increased feeding is the result of autotrophic energy supply that is available to support metabolically demanding heterotrophic processes, and (2) increased heterotrophic contribution is critical to the assimilation of photosynthetic carbon into host biomass. Both explanations are likely associated with respiratory demand. In particular, prey digestion is an energy-demanding process that increases metabolism (Sebens, 2002) and requires photosynthetically fixed carbon to support animal respiration (Falkowski et al., 1984). If autotrophic energy exceeds respiratory demand and heterotrophically derived carbon is available, then autotrophic carbon may be combined with heterotrophic energy and elements such as nitrogen and phosphorous to build host biomass (Dubinsky and Jokiel, 1994; Hoogenboom et al., 2010). This mechanism driven by respiratory demand is supported by the differential fate of carbon in symbiotic cnidarians: photosynthetically fixed carbon is quickly respired by the

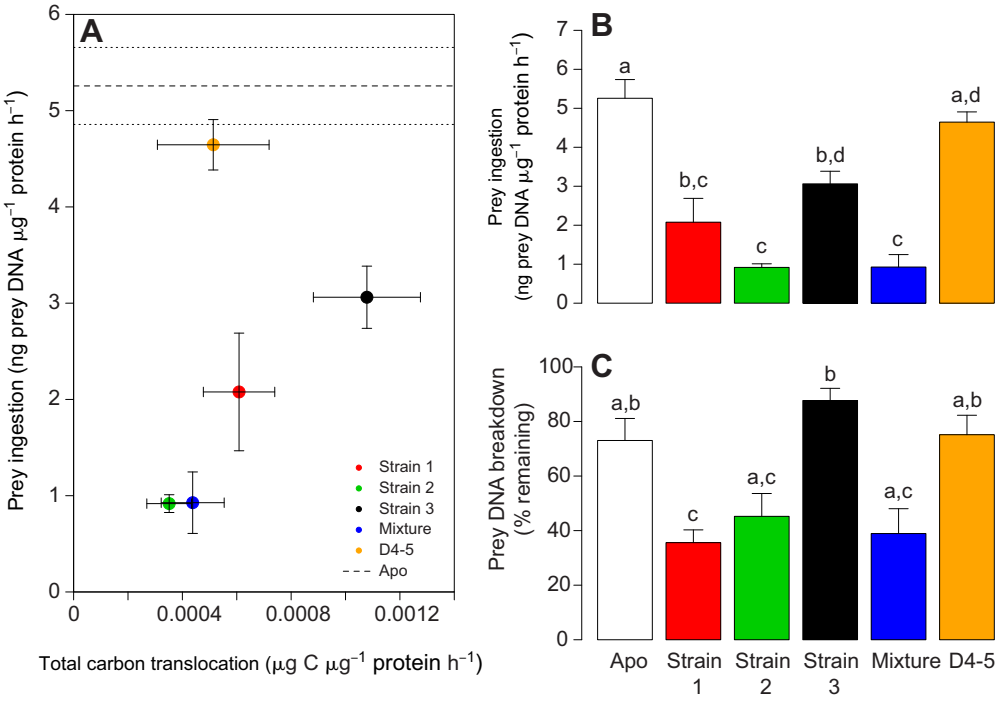

Fig. 2. Autotrophy and heterotrophy. Autotrophy and heterotrophy were measured in individuals (*N*=5) hosting a single unique strain of *S. minutum* (denoted by strain 1, 2 or 3), a mixture of *S. minutum* (strain 2) and *S. psygmophilum*, or *Symbiodinium* D4-5. (A) Total carbon translocation and prey ingestion rates (means±s.e.). Apo denotes aposymbiotic anemones (mean, dashed line; s.e., dotted lines). (B) Prey ingestion rate (means±s.e.; estimated through prey DNA content). (C) Prey DNA breakdown at ingestion (means±s.e.; 100% indicates no prey DNA breakdown and 0% indicates total prey DNA breakdown). Different superscript letters in B and C indicate significant differences among genotypes (Tukey's HSD, P<0.05). Symbioses with strains 1, 2, 'mixture' and D4-5 and the aposymbiotic animals were all with the same clonal (CC7) anemone line.

The Journal of Experimental Biology (2015) 218, 858-863 doi:10.1242/jeb.115519

animal host, whereas heterotrophically derived carbon is incorporated more into animal biomass such as phospholipids, proteins and nucleic acids (Bachar et al., 2007). The increased prey ingestion observed in strain 3 thus follows the positive association between autotrophy and heterotrophy (Fig. 2A). However, the reduced prey breakdown observed for this same strain differs from that of anemones hosting *S. minutum*, i.e. strain 1, 2 and mixture, and is similar to results observed in aposymbiotic and D4-5 anemones (Fig. 2C). This may be a consequence of physiological differences among different host genetic lines. Different lines of anemones may have physiological differences that slow down digestion or different morphological features, as previously detailed, that increase prey capture rate (Hiebert and Bingham, 2012). In contrast, as the same host line was used in all anemones apart from strain 3, the increased prey ingestion with slower digestion in aposymbiotic and D4-5 anemones is associated with the absence of symbionts or the type of symbiont, respectively. This suggests that heterotrophy is a partial energetic sink in itself due to absent or insufficient carbon from autotrophy to support animal metabolism. Such quantitative and qualitative differences may have implications for energy budgets of the symbiosis. Further, widely used models quantifying autotrophic and heterotrophic contributions to animal respiration, known as CZAR (Muscatine et al., 1981) and CHAR (Grottoli et al., 2006) respectively, may need to be adjusted to account for different *Symbiodinium* types and the important metabolic costs of feeding and digestion. Likewise, as isolating the respiratory contribution from the algal and animal components within intact symbioses is impossible, such models and their underlying assumptions may not provide the necessary detail to tease apart such differences as noted here.

In conclusion, heterotrophy is positively associated with autotrophy, and the latter is significantly correlated with the symbionts' capacity to fix and translocate carbon in a density-dependent manner. Physiological variability within a single *Symbiodinium* species thus results in a change in the nutritional status of the cnidarian host where both autotrophy and heterotrophy play a pivotal role. The influence of symbiont type in contributing to this trade-off in trophic patterns is especially important in the context of coral bleaching events, as not all stable dinoflagellate/animal symbioses are equally nutritionally advantageous to the animal. Bleached corals may increase their feeding rates (Grottoli et al., 2006; Hughes and Grottoli, 2013; Leal et al., 2014a) but may not take advantage of such opportunities if host metabolic processes associated with prey digestion are affected by symbiont competency and consequent autotrophic capacity. *Symbiodinium* functional diversity that extends below the species level is thus critical to the nutritional plasticity of cnidarian–dinoflagellate symbioses, influencing their resilience and acclimation, and having ecological implications for the success of these symbioses in marine environments.

MATERIALS AND METHODS

Animal models

Anemones consisted of a monoclonal line of aposymbiotic (Burriesci et al., 2012) *A. pallida* (clone CC7) (provided by J. Pringle, Stanford University, USA). Aposymbiotic anemones were kept in constant darkness over 2 years in a closed system containing filtered seawater (FSW, 1 µm) and fed brine shrimp weekly. Different combinations of *A. pallida* symbioses were generated by infecting aposymbiotic anemones [similar to Schoenberg and Trench (1980), minus the seawater extract of *Artemia*] with genetically distinct cultures of *Symbiodinium* originating from various symbiotic cnidarians (supplementary material Table S3). Two of the symbionts used were recently described species of clade B *Symbiodinium*, *S. minutum* and *S. psygmophilum* (Lajeunesse et al., 2012), while the third, D4-5, represents a stress-tolerant clade of symbionts (Glynn et al., 2001; Lajeunesse et al., 2010b). Three strains (designated as strains 1, 2 and 3) of the species *S. minutum* (ITS2 type B1) were chosen because they are the dominant symbiont of wild *Aiptasia pallida* (Thornhill et al., 2013). A mixture of *S. minutum* (ITS2 type B1) with *S. psygmophilum* (ITS2 type B2) was also included to investigate the effects of a mixed symbiont infection between two species within the same clade. Another monoclonal line of *A. pallida*, originally collected in Bermuda, was used as well and hosted one of the unique strains of *S. minutum* (strain 3). All associations of *A. pallida* symbiosis were stable for over 1 year and kept in flow-through systems using FSW under normal growth conditions (26°C, ~33‰, 150 µmol photons m^{-2} s^{-1} photosynthetic photon flux, 12 h light–dark cycle) and fed brine shrimp weekly (Leal et al., 2012). Associations with each symbiont's genotype were confirmed before experiments (see below). Aposymbiotic anemones were confirmed to be free of dinoflagellates by periodic microscopic examination as well as after shifting several anemones into lighted incubators over several months.

Genetic identification of *Symbiodinium* types

One representative anemone from each of the five *Symbiodinium* combinations was sampled from batch isoclonal cultures prior to the experiment to confirm the genetic identity of the symbionts. Following the heterotrophic feeding (see below), symbiont identity was again confirmed for all five replicates per host–symbiont combination by extracting total DNA from 100 µl of the anemone homogenate (LaJeunesse, 2002). The partial 5.8S and ITS2 region of each sample was fingerprinted using PCR-DGGE and the fingerprints characterized by Sanger sequencing of the fingerprint (LaJeunesse, 2002). The symbionts, and their corresponding ITS2 fingerprints, used in this study are detailed in supplementary material Table S3. Addition diversity and resolution within the B1 ITS2 lineage that better approximates species-level diversity can be gained by sequencing the microsatellite locus B7Sym15 (Finney et al., 2010; Lajeunesse et al., 2012). Therefore, the three strains used were characterized based on the flanker region sequence of this locus to definitively place them within the species *S. minutum* (matching GenBank accession no. JX263427). To further elucidate the genetic diversity within *S. minutum* and characterize each strain (i.e. multilocus genotype) used in this study, fragment analysis was conducted on five microsatellite loci (B7Sym15, B7Sym34, B7Sym36, CA4.86 and CA6.38) for the samples prior to the experiment (supplementary material Table S4) (Santos and Coffroth, 2003; Pettay and LaJeunesse, 2007). Two of these loci (B7Sym15 and B7Sym36) were further used at the conclusion of the feeding experiment (see below) to confirm the identity of the genetically distinct *S. minutum* strains and verify that the symbioses had remained stable at both the ITS2 and strain level. Lastly, to verify that the *Aiptasia* clones were genetically distinct, fragment analysis was conducted on six microsatellite loci (AIPT6, AIPT8, AIPT14, AIPT15, AIPT17 and AIPT20) developed for *Aiptasia* spp. Briefly, microsatellite loci were developed from EST sequences of *A. pallida* (Sunagawa et al., 2009) that were vector screened (using VecScreen and the UniVec NCBI vector library) and assembled (CAP3) (Huang and Madan, 1999). Contigs and singlet sequences were screened for simple sequence repeat (SSR) of di-, tri-, tetra-, penta- and hexa-nucleotides with more than six repeats [WebSat (Martins et al., 2009)]. Primers were designed for candidate loci [Primer3 (Rozen and Skaletsky, 2000)] and the loci screened on *A. pallida* samples from the Florida Keys and Bermuda collected in 2011. The two clones used in this study differed by at least one allele at all loci except AIPT14, proving that the clonal lines are genetically different (supplementary material Table S5).

Carbon uptake and translocation

Starved anemones of each *Symbiodinium* combination genotype were placed in separate 7 ml scintillation vials containing 2 ml of seawater spiked with 15 µl of ^{14}C bicarbonate (specific activity 17 µCi $µmol^{-1}$) following previously described procedures (Davy and Cook, 2001). Five anemones were used for each *Symbiodinium* combination and treatment. All vials were then placed on an LED light-table (Cool White Cree XPG-R5; 150 µmol photons m^{-2} s^{-1}; 28°C) for 90 min. Two additional anemones from each *Symbiodinium* combination were placed in vials with spiked seawater and maintained in the dark for 90 min to account for carbon uptake in the dark.

The Journal of Experimental Biology (2015) 218, 858-863 doi:10.1242/jeb.115519

Three additional vials containing only the spiked seawater were also included for measurement of total activity. After incubation, each anemone was ground in 1 ml of seawater with a 1.5 ml Ten Broeck tissue grinder. A 100 µl sample of the resulting homogenate was removed and fixed with 10 µl of 1% glutaraldehyde (Acros Organics) and utilized for symbiont cell counts (see below). The remaining homogenate was centrifuged at 5000 ***g*** for 5 min to separate the host and symbiont portions. A 500 µl sample of the host supernatant (HS) was removed and the remaining supernatant was stored for downstream calculation of protein content. The symbiont pellet (S) was then resuspended in 400 µl of FSW. Dissolved organic carbon (DOC) released from the organism was also calculated by removing 200 µl of seawater from each anemone-containing vial. All samples were acidified using an equal volume of 2 mol l^{-1} HCL for 24 h, then dosed with 5 ml of scintillation cocktail. After an additional 24 h period, radioactivity was determined with a liquid scintillation counter (Beckman LS-6500). Calculations were made using the mean specific activity (gC dpm^{-1}), which was estimated from the carbon content of 0.024 g C l^{-1} of seawater (Davy and Cook, 2001). All samples were background and dark uptake corrected. Translocation (T) was calculated as (DOC+HS) normalized to host protein (see below). Photosynthesis (P_{net}) was calculated as (DOC+HS+S) normalized to total symbiont cells per anemone (see below). The fraction of photosynthate translocated to the host was calculated as (DOC+HS)/(DOC+HS+S).

Heterotrophic feeding

Aiptasia pallida individuals starved over 1 week were placed in 1.2 l Plexiglas chambers with unidirectional flow (0.1 m s^{-1}) (Leal et al., 2014b) and each replicate consisted of a separate feeding chamber with one individual each for each symbiont genotype tested and aposymbiotic anemones. Newly hatched *Artemia* nauplii (24 h) were added at a final concentration of 2 nauplii ml^{-1} to each chamber once the polyps were expanded. After 15 min feeding time, anemones were sampled and thoroughly rinsed three times in FSW to detach any prey that were captured but not ingested. Five individuals were immediately flash-frozen and stored at −80°C for molecular assessment of prey ingestion, and the other five individuals were transferred to a prey-free environment where they were allowed to digest ingested prey over 24 h before sampling as previously described. Unfed *A. pallida* from each *Symbiodinium* combination were also sampled prior to feeding incubations as negative controls. Samples (N=5) of a known number of *Artemia* nauplii (varying from 5 to 100 individuals) used in the experiment were also flash-frozen and stored at −80°C for genomic DNA extraction.

Each individual stored during feeding incubations was thawed at room temperature, ground with Ultra-Turrax (IKA, Staufen, Germany) in 1 ml of FSW, and 300 µl transferred for genomic DNA extraction. The remaining 700 µl were centrifuged (5 min, 4°C, 8000 ***g***) to pellet the symbionts. The supernatant composed of the cnidarian host fraction was transferred to a new tube and stored at −80°C for later protein quantification. The pellet was re-suspended in 400 µl of FSW and 100 µl was aliquoted to a new tube with 10 µl of glutaraldehyde (1%, Acros Organics) and stored at 4°C for determination of symbiont cell densities.

Total animal protein was assessed using Pierce BCA Protein Assay Kit (Thermo Scientific, Rockford, IL, USA) following the manufacturer's instructions for microplate readings. Absorbance (562 nm) was measured using a FluoStar Omega reader (BMG Labtech GmbH, Ortenberg, Germany). Symbiont cell density was recorded by fluorescence microscopy. Six independent replicate counts were performed for each sample on a hemocytometer. Samples were photographed using a Nikon microphot-FXA epifluorescence microscope (100× magnification). Photographs were then analyzed by ImageJ software (Schneider et al., 2012) with the analyze particles function.

Extraction of genomic DNA was performed using the MoBio UltraClean Tissue and Cells DNA Isolation Kit (Carlsbad, CA, USA) following the manufacturer's instructions, apart from the bead beating step, which used ∼100 µl of 0.5 mm glass beads for each extraction. After extraction, genomic DNA was quantified using a Nanodrop 2000c spectrophotometer (Thermo Scientific). Total genomic DNA from *Artemia* nauplii samples was used to estimate the genomic DNA content per individual prey item (Leal et al., 2014b). Prey DNA content in each anemone sample was estimated through qPCR amplification of *Artemia* DNA using the primers Af18s-1298F and Af18S-1373R (Leal et al., 2014b). For each qPCR reaction, a dilution series of extracted genomic DNA from *Artemia* nauplii was run as a quantitative standard. The appropriate amount of template DNA in all assays was achieved using 1 µl of genomic DNA extract. qPCR reactions were performed using a 7500 RealTime PCR System (Applied Biosystems, Foster City, CA, USA) in 96-well plates with each reaction well containing 5 µl of SensiMix SYBR Hi-ROX reaction mix (Bioline, UK), 400 nmol l^{-1} of primers and template genomic DNA. Amplification conditions included an initial denaturation step (10 min, 95°C) followed by 40 amplification cycles (15 s, 94°C; 30 s 60°C annealing/extension temperature). Each reaction was followed by a melt-curve thermal profile from 60°C to 95°C to evaluate specificity of the primers. All reactions were run in triplicate and PCR-grade water was used as a template for negative control, as well as genomic DNA from unfed anemones. Mean primer efficiency in all qPCR reactions was 99.2±1.0%. To estimate prey DNA breakdown, all samples were also run in qPCR reactions using primers Af18s-1298F and Af18S-1422R (Leal et al., 2014b). As prey is digested, there is a decreasing quantity of genomic DNA with increasing amplicon size (Troedsson et al., 2009). Thus, the ratio between prey DNA content obtained with the two primer sets amplifying amplicon sizes of 73 and 112 bp will be 0 if all prey DNA is degraded (no prey DNA detected using the primer set amplifying the 112 bp amplicon) and 100 if no prey DNA is broken down (equal amount of prey DNA detected using the two primer sets) (Leal et al., 2014b). Percentage digestion rate was assessed through the ratio between prey DNA content detected in samples collected after 24 h digestion and immediately after ingestion. A digestion rate of 0% indicates that no prey DNA was detected after 24 h digestion, whereas 100% means identical prey DNA contents are observed immediately after ingestion and after 24 h digestion. Prey DNA content was normalized to animal protein.

Statistics

All measured parameters were compared among host–dinoflagellate combinations with a one-way ANOVA. Tukey's HSD *post hoc* test was used when statistical differences were observed (P<0.05). Pearson's correlation was used to assess the relationship between different parameters measured in the same *Aiptasia* individuals. Because of the necessarily destructive nature of the methods, carbon translocation and prey ingestion were measured on different individuals; hence, some statistical comparisons were not possible. Patterns of symbiont genotype and photosynthesis or symbiont cell density on carbon translocation per cell or per unit host protein, respectively, were tested using ANCOVA. Model residuals were checked to verify assumptions of normality and homogeneity of variance, and transformations were not required (Zuur et al., 2009). Statistical analyses were performed with R (R Development Core Team, 2013).

Acknowledgements

The authors would like to thank J. Pringle (Stanford University) for the CC7 *A. pallida* clone, and two anonymous reviewers for their comments and suggestions to improve the manuscript.

Competing interests

The authors declare no competing or financial interests.

Author contributions

M.C.L., K.H., D.T.P., A.G. and M.E.W. designed the research, M.C.L., K.H. and D.T.P. performed the research and analyzed the data, A.G. and M.E.W. contributed new reagents/analytic tools, M.C.L., K.H., D.T.P., R.C. and M.E.W. wrote the manuscript.

Funding

M.C.L. was supported by a PhD scholarship (SFRH/BD/63783/2009) funded by the Fundação para a Ciência e Tencologia (QREN-POPH-Type 4.1-Advanced Training, subsidized by the European Social Fund and National Ministério da Educação e Ciência funds). This work was supported by project SYMBIOCoRe (|FP7-PEOPLE-2011-IRSES, 295191) and by the National Science Foundation (IOS 1258065, EF 1316055 and ED 1040940).

Supplementary material

Supplementary material available online at
http://jeb.biologists.org/lookup/suppl/doi:10.1242/jeb.115519/-/DC1

References

Anthony, K. R. N. and Fabricius, K. E. (2000). Shifting roles of heterotrophy and autotrophy in coral energetics under varying turbidity. *J. Exp. Mar. Biol. Ecol.* **252**, 221-253.

Bachar, A., Achituv, Y., Pasternak, Z. and Dubinsky, Z. (2007). Autotrophy versus heterotrophy: the origin of carbon determines its fate in a symbiotic sea anemone. *J. Exp. Mar. Biol. Ecol.* **349**, 295-298.

Burriesci, M. S., Raab, T. K. and Pringle, J. R. (2012). Evidence that glucose is the major transferred metabolite in dinoflagellate-cnidarian symbiosis. *J. Exp. Biol.* **215**, 3467-3477.

Coffroth, M. A. and Santos, S. R. (2005). Genetic diversity of symbiotic dinoflagellates in the genus *Symbiodinium*. *Protist* **156**, 19-34.

Davy, S. and Cook, C. (2001). The relationship between nutritional status and carbon flux in the zooxanthellate sea anemone *Aiptasia pallida*. *Mar. Biol.* **139**, 999-1005.

Dubinsky, Z. and Berman-Frank, I. (2001). Uncoupling primary production from population growth in photosynthesizing organisms in aquatic ecosystems. *Aquat. Sci.* **63**, 4-17.

Dubinsky, Z. and Jokiel, P. L. (1994). Ratio of energy and nutrient fluxes regulates symbiosis between zooxanthellae and corals. *Pacific Sci.* **48**, 313-324.

Fabina, N. S., Putnam, H. M., Franklin, E. C., Stat, M. and Gates, R. D. (2013). Symbiotic specificity, association patterns, and function determine community responses to global changes: defining critical research areas for coral-*Symbiodinium* symbiosis. *Global Change Biol.* **19**, 3306-3316.

Falkowski, P., Dubinsky, Z., Muscatine, L. and Porter, J. W. (1984). Light and the bioenergetics of a symbiotic coral. *BioScience* **34**, 705-709.

Ferrier-Pagès, C., Peirano, A., Abbate, M., Cocito, S., Negri, A., Rottier, C., Riera, P., Rodolfo-Metalpa, R. and Reynaud, S. (2011). Summer autotrophy and winter heterotrophy in the temperate symbiotic coral *Cladocora caespitosa*. *Limnol. Oceanogr.* **56**, 1429-1438.

Finney, J. C., Pettay, D. T., Sampayo, E. M., Warner, M. E., Oxenford, H. A. and LaJeunesse, T. C. (2010). The relative significance of host-habitat, depth, and geography on the ecology, endemism, and speciation of coral endosymbionts in the genus *Symbiodinium*. *Microb. Ecol.* **60**, 250-263.

Glynn, P. W., Maté, J. L., Baker, A. C. and Calderón, M. O. (2001). Coral bleaching and mortality in Panama and Ecuador during the 1997-1998 El Niño-southern oscilation event: spatial/temporal patterns and comparisons with the 1982-1983 event. *Bull. Mar. Sci.* **69**, 79-109.

Grottoli, A. G., Rodrigues, L. J. and Palardy, J. E. (2006). Heterotrophic plasticity and resilience in bleached corals. *Nature* **440**, 1186-1189.

Grottoli, A. G., Warner, M. E., Levas, S. J., Aschaffenburg, M. D., Schoepf, V., McGinley, M., Baumann, J. and Matsui, Y. (2014). The cumulative impact of annual coral bleaching can turn some coral species winners into losers. *Global Change Biol.* **20**, 3823-3833.

Hiebert, T. C. and Bingham, B. L. (2012). The effects of symbiotic state on heterotrophic feeding in the temperate sea anemone *Anthopleura elegantissima*. *Mar. Biol.* **159**, 939-950.

Hoogenboom, M., Rodolfo-Metalpa, R. and Ferrier-Pages, C. (2010). Co-variation between autotrophy and heterotrophy in the Mediterranean coral *Cladocora caespitosa*. *J. Exp. Biol.* **213**, 2399-2409.

Huang, X. and Madan, A. (1999). CAP3: a DNA sequence assembly program. *Genome Res.* **9**, 868-877.

Hughes, A. D. and Grottoli, A. G. (2013). Heterotrophic compensation: a possible mechanism for resilience of coral reefs to global warming or a sign of prolonged stress? *PLoS ONE* **8**, e81172.

LaJeunesse, T. (2002). Diversity and community structure of symbiotic dinoflagellates from Caribbean coral reefs. *Mar. Biol.* **141**, 387-400.

Lajeunesse, T. C., Pettay, D. T., Sampayo, E. M., Phongsuwan, N., Brown, B., Obura, D., Hoegh-Guldberg, O. and Fitt, W. K. (2010a). Long-standing environmental conditions, geographic isolation and host-symbiont specificity influence the relative ecological dominance and genetic diversification of coral endosymbionts in the genus *Symbiodinium*. *J. Biogeography* **37**, 785-800.

Lajeunesse, T. C., Smith, R., Walther, M., Pinzon, J., Pettay, D. T., McGinley, M., Aschaffenburg, M., Medina-Rosas, P., Cupul-Magana, A. L., Perez, A. L. et al. (2010b). Host-symbiont recombination versus natural selection in the response of coral-dinoflagellate symbioses to environmental disturbance. *Proc. R. Soc. Lond. B Biol. Sci.* **277**, 2925-2934.

Lajeunesse, T. C., Parkinson, J. E. and Reimer, J. D. (2012). A genetics-based description of *Symbiodinium minutum* sp. nov. and *S. psygmophilum* sp. nov. (Dinophyceae), two dinoflagellates symbiotic with cnidaria. *J. Phycol.* **48**, 1380-1391.

Leal, M. C., Nunes, C., Engrola, S., Dinis, M. T. and Calado, R. (2012). Optimization of monoclonal production of the glass anemone *Aiptasia pallida* (Agassiz in Verrill, 1864). *Aquaculture* **354-355**, 91-96.

Leal, M. C., Nunes, C., Kempf, S., Reis, A., da Silva, T. L., Serôdio, J., Cleary, D. F. R. and Calado, R. (2013). Effect of light, temperature and diet on the fatty acid profile of the tropical sea anemone *Aiptasia pallida*. *Aquacult. Nutr.* **19**, 818-826.

Leal, M. C., Ferrier-Pagès, C., Calado, R., Brandes, J. A., Frischer, M. E. and Nejstgaard, J. C. (2014a). Trophic ecology of the facultative symbiotic coral *Oculina arbuscula*. *Mar. Ecol. Prog. Ser.* **504**, 171-179.

Leal, M. C., Nejstgaard, J. C., Calado, R., Thompson, M. E. and Frischer, M. E. (2014b). Molecular assessment of heterotrophy and prey digestion in zooxanthellate cnidarians. *Mol. Ecol.* **23**, 3838-3848.

Loram, J. E., Trapido-Rosenthal, H. G. and Douglas, A. E. (2007). Functional significance of genetically different symbiotic algae *Symbiodinium* in a coral reef symbiosis. *Mol. Ecol.* **16**, 4849-4857.

Martins, W. S., Lucas, D. C. S., Neves, K. F. S. and Bertioli, D. J. (2009). WebSat: a web software for microsatellite marker development. *Bioinformation* **3**, 282-283.

Muscatine, L., McCloskey, L. and Marian, R. (1981). Estimating the daily contribution of carbon from zooxanthellae to coral animal respiration. *Limnol. Oceanogr.* **26**, 601-611.

Muscatine, L., Porter, J. W. and Kaplan, I. R. (1989). Resource partitioning by reef corals as determined from stable isotope composition. *Mar. Biol.* **100**, 185-193.

Pettay, D. T. and LaJeunesse, T. C. (2007). Microsatellites from clade B *Symbiodinium* spp. specialized for Caribbean corals in the genus *Madracis*. *Mol. Ecol. Notes* **7**, 1271-1274.

R Development Core Team. (2013). R: a language and environment for statistical computing (ed. R Foundation for Statistical Computing). Vienna, Austria: R Foundation for Statistical Computing. http://www.R-project.org

Rowan, R. (2004). Coral bleaching: thermal adaptation in reef coral symbionts. *Nature* **430**, 742.

Rozen, S. and Skaletsky, H. (2000). Primer 3 on the WWW for general users and for biologist programmers. *Methods Mol. Biol.* **132**, 365-386.

Sampayo, E., Ridgway, T., Bongaerts, P. and Hoegh-Guldberg, O. (2008). Bleaching susceptibility and mortality of corals are determined by fine-scale differences in symbiont type. *Proc. Natl. Acad. Sci. USA* **105**, 10444-10449.

Santos, S. R. and Coffroth, M. A. (2003). Molecular genetic evidence that dinoflagellates belonging to the genus *Symbiodinium* Freudenthal are haploid. *Biol. Bull.* **204**, 10-20.

Schneider, C., Rasband, W. S. and Eliceiri, K. W. (2012). NIH Image to ImageJ: 25 years of image analysis. *Nat. Methods* **9**, 671-675.

Schoenberg, D. A. and Trench, R. K. (1980). Genetic variation in *Symbiodinium* (=*Gymnodinium*) *microadriaticum* Freudenthal, and specificity in its symbiosis with marine invertebrates: III. Specificity and infectivity of *Symbiodinium microadriaticum*. *Proc. Natl. Acad. Sci. USA* **207**, 445-460.

Sebens, K. P. (2002). Energetic constraints, size gradients, and size limits in benthic marine invertebrates. *Integr. Comp. Biol.* **42**, 853-861.

Smith, G. and Muscatine, L. (1999). Cell cycle of symbiotic dinoflagellates: variation in G1 phase-duration with anemone nutritional status and macronutrient supply in the *Aiptasia pulchella-Symbiodinium pulchrorum* symbiosis. *Mar. Biol.* **134**, 405-418.

Starzak, D. E., Quinnell, R. G., Nitschke, M. R. and Davy, S. K. (2014). The influence of symbiont type on photosynthetic carbon flux in a model cnidarian-dinoflagellate symbiosis. *Mar. Biol.* **161**, 711-724.

Sunagawa, S., Wilson, E. C., Thaler, M., Smith, M. L., Caruso, C., Pringle, J. R., Weis, V. M., Medina, M. and Schwarz, J. A. (2009). Generation and analysis of transcriptomic resources for a model system on the rise: the sea anemone *Aiptasia pallida* and its dinoflagellate endosymbiont. *BMC Genomics* **10**, 258.

Thornhill, D. J., Xiang, Y., Pettay, D. T., Zhong, M. and Santos, S. R. (2013). Population genetic data of a model symbiotic cnidarian system reveal remarkable symbiotic specificity and vectored introductions across ocean basins. *Mol. Ecol.* **22**, 4499-4515.

Tremblay, P., Grover, R., Maguer, J. F., Hoogenboom, M. and Ferrier-Pagès, C. (2014). Carbon translocation from symbiont to host depends on irradiance and food availability in the tropical coral *Stylophora pistillata*. *Coral Reefs* **33**, 1-13.

Troedsson, C., Simonelli, P., Nägele, V., Nejstgaard, J. C. and Frischer, M. E. (2009). Quantification of copepod gut content by differential length amplification quantitative PCR (dla-qPCR). *Mar. Biol.* **156**, 253-259.

Venn, A. A., Loram, J. E. and Douglas, A. E. (2008). Photosynthetic symbioses in animals. *J. Exp. Bot.* **59**, 1069-1080.

Weis, V. M., Davy, S. K., Hoegh-Guldberg, O., Rodriguez-Lanetty, M. and Pringle, J. R. (2008). Cell biology in model systems as the key to understanding corals. *Trends Ecol. Evol.* **23**, 369-376.

Zuur, A. F., Ieno, E. N., Walker, N. J., Saveliev, A. A. and Smith, G. M. (2009). *Mixed Effects Models and Extensions in Ecology with R*. New York: Springer.

Table S1. Summary statistics for slopes from multiple linear regressions of carbon translocation as a function of photosynthesis or symbiont density.

Carbon translocation (µg C cell^{-1} h^{-1})				Total carbon translocation (µg C host protein^{-1} h^{-1})		
	F value	*P* value			*F* value	*P* value
Photosynthesis (µC cell^{-1} hour^{-1})	388.89	< 0.001		Cell density (cells µg^{-1} protein)	35.93	< 0.001
Symbiont genotype	6.81	< 0.01		Symbiont genotype	1.48	0.26
Interaction	12.77	< 0.001		Interaction	1.76	0.19
Residual d.f.	15			Residual d.f.	15	
	Slope (β)	*P* value			Slope (β)	*P* value
(Intercept)	3.01 x 10^{-8}	0.71		(Intercept)	-2.29 x 10^{-4}	0.57
Cell density	2.76 x 10^{-1}	< 0.05		Cell density	3.02 x 10^{-7}	< 0.05
Strain 2	-7.12 x 10^{-8}	0.41		Strain 2	1.79 x 10^{-4}	0.87
Strain 3	-4.89 x 10^{-8}	0.58		Strain 3	7.57 x 10^{-4}	0.41
Mixture	3.15 x 10^{-8}	0.72		Mixture	4.37 x 10^{-4}	0.49
D4-5	2.73 x 10^{-7}	< 0.01		D4-5	-3.13 x 10^{-4}	0.53
Cell density * Strain 2	3.57 x 10^{-1}	< 0.05		Cell density * Strain 2	-1.44 x 10^{-7}	0.74
Cell density * Strain 3	9.39 x 10^{-2}	0.42		Cell density * Strain 3	-1.93 x 10^{-7}	0.37
Cell density * Mixture	1.28 x 10^{-2}	0.92		Cell density * Mixture	-2.39 x 10^{-7}	0.42
Cell density * D4-5	-2.36 x 10^{-1}	< 0.05		Cell density * D4-5	2.71 x 10^{-7}	0.16

Table S2. Prey digestion of individuals hosting a single unique genotype of *Symbiodinium minutum* (strain 1, 2 and 3), a mixture of one genotype of *S. minutum* and *S. psygmophilum* (mixture) or *Symbiodinium* D4-5, and aposymbiotic anemones.

Prey digestion	Strain 1	Strain 2	Strain 3	Mixture	D4-5	Aposymbiotic
Artemia DNA present 24h after ingestion (%)	0.6	0.2	3.7	0.8	2.4	8.0

Prey digestion is estimated as the ratio between prey DNA content 24 h after ingestion and immediately after ingestion (n = 5; 100% denotes no prey digestion and 0% total prey digestion).

Table S3. Culture name, cnidarian host from which the symbionts were obtained and corresponding ITS2 Genbank numbers for the different symbiont strains.

Symbiont	Culture name	Host	Corresponding ITS2 Genbank #
Symbiodinium minutum strain 1	FLAp2	*Aiptasia pallida*	AF333511
Symbiodinium minutum strain 2	Unknown	Unknown	AF333511
Symbiodinium minutum strain 3	N/A	*Aiptasia pallida*	AF333511
Symbiodinium psygmophilum	Unknown	Unknown	AF333512
Symbiodinium clade D4-5	Ap31	Unknown anemone	AF499802 (4) EU812743 (5)

Table S4. Alleles for the five *Symbiodinium* clade B microsatellites used to resolve strain diversity.

Strain or MLG	Microsatellite Loci				
	B7Sym15	**B7Sym34**	**BySym36**	**CA4.86**	**CA6.38**
Symbiodinium minutum strain 1	263	281	196	182	101
Symbiodinium minutum strain 2	263	267	163	199	103
Symbiodinium minutum strain 3	259	271	169	182	101
Symbiodinium minutum + *S. psygmophilum*[a]	263	267	163	199	103

[a] Microsatellites loci for the *S. minutum* strain present in the mixture with *S. psygmophilum*.

Table S5. Alleles for the six *Aiptasia* microsatellites used to resolve clone diversity.

***Aiptasia* clone**	**Microsatellite Loci**					
	AIPT6	**AIPT8**	**AIPT14**	**AIPT15**	**AIPT17**	**AIPT20**
CC7	302	293	188	319	292	334
	302	295	191	322	292	334
Bermudas	302	293	188	319	294	339
	318	293	191	319	296	341